Robust controller design for turning operations based on measured frequency response functions

David Hajdu *, **Tamas Insperger** ** **and Gabor Stepan** *

* *Budapest University of Technology and Economics, 1111 Budapest, Hungary (e-mail: hajdu@mm.bme.hu, stepan@mm.bme.hu).*
** *Department of Applied Mechanics, Budapest University of Technology and Economics and MTA-BME Lendület Human Balancing Research Group, 1111 Budapest, Hungary (e-mail: insperger@mm.bme.hu).*

Abstract: One of the most significant limitation of the productivity of machining operations is the regenerative machine tool vibration, also called machine tool chatter, which is a self-excited vibration between the tool and the workpiece induced by the chip formation mechanism. Extension of the chatter-free parameters is possible by active chatter control techniques. The design of the controller requires the identification of the dynamic properties of the system. Uncertainties in the system parameters may result in an inappropriate control performance. Robust control design is therefore a necessary step during the optimization of machining operations. In this paper, a fast and efficient method is presented to determine the region of control gains in the presence of uncertainties in the measured frequency response functions. The method is based on the concept of structured singular values.

Keywords: Stability of delay systems, Robust control, Robust time-delay systems, Machining, Structured singular value

1. INTRODUCTION

Stability of machining operations is a key problem in efficiency oriented industrial applications. Machine tool vibration, also called machine tool chatter, sets strong limitation to the optimization of material removal rate, therefore reduces the productivity and increases machining costs. Techniques to suppress machine tool chatter is therefore an important task in machining engineering.

The first mathematical models describing machine tool chatter were published in the works of Tobias (1965), Tlusty and Spacek (1954). Since then, the so-called regenerative effect has become the most widely accepted explanation for machine tool vibration. As the tool vibrates, its motion is copied onto the surface of the material and affects the removable chip thickness one revolution later. The mathematical model of the phenomenon involves a delayed feedback mechanism via the dependence of the cutting force on the variation of the chip thickness. From the dynamic system's point of view, chatter is associated with the loss of stability of the stationary (chatter-free) machining process followed by a large amplitude self-excited vibration between the tool and the workpiece.

Stability properties of machining processes are depicted by the so-called stability lobe diagrams, which plot stable domains in the plane of machining parameters, usually the spindle speed and the depth of cut. This provides a guide to the machinists to avoid chatter by selecting optimal technological parameters. The calculation of conventional stability lobe diagrams include the properties of the workpiece material, such as cutting force characteristics, and the dynamical properties of the tool, which are usually measured via impact tests. Identification of system parameters, however, are always affected by noise and uncertainties, therefore stability predictions often do not match experimental validations. Uncertainty and robust analysis therefore plays an important role in stability predictions in order to guarantee stable operation.

There are several studies related to robust stability analysis of machine tool chatter. The edge theorem combined with the zero exclusion method is presented by Park and Qin (2007), while Totis (2009) has introduced the RCPM method for robust stability predictions in milling processes. Both techniques, similarly to many others, require the uncertainty bound of the system parameters and limited to low number of uncertain parameters due to extensive calculation time. With the use of local and global sensitivity methods, the probability of stability can be approximated based on the moments of the probability distribution functions. Studies related to this field are presented by Huang et al. (2016a) for turning operations and by Huang et al. (2016b) for milling operations. A different approximate solution is given by Löser and Großmann (2016), which provides confidence levels of stability boundaries for high number of perturbed parameters. A completely frequency-domain-based solution is proposed by Hajdu et al. (2016) for turning operations, which re-

quires no fitted modal parameters, only the uncertainty of the measured frequency response functions.

In order to extend the domain of stable parameters and suppress machine tool chatter, several engineering applications have been presented. For instance, a vibration absorber is presented by Sims (2007), an impedance modulation technique by Segalman and Butcher (2000) and a self-tuning dynamic vibration absorber by Aguirre et al. (2013). An adaptive chatter suppression technique is proposed by van Dijk et al. (2008), which is based on a real-time chatter detection and automatic spindle speed adjustment. A Pyragas-type feedback control is presented by van de Wouw et al. (2015) to mitigate chatter in high-speed milling. A chatter control is also introduced by van Dijk et al. (2010) based on the structured singular values, where the spindle speed and depth of cut are treated as uncertain parameters in order to enlarge the domain of stable machining parameters. A PD controller based chatter suppression method for turning operations is presented by Lehotzky and Insperger (2012), where actuation and measurement are utilized theoretically at the tool tip.

One of the most typical drawback of each robust stability analysis techniques is that the computation time increases with the number of uncertain parameters. The calculation of the robust stability boundaries based on the structured singular values (μ-values) has been found an efficient tool in many engineering applications. Still the accurate approximation of the μ-values is often time-consuming and leads to a badly scaled mathematical problem. In this paper, based on the results of Karow et al. (2006), a fast and efficient method is presented in order to overcome the problem of high computation time. The mechanical model under analysis describes a turning operation subjected to a PD control with feedback delay. It is assumed that the control force is acting near the tool tip. The dynamical properties of the tool are given by a frequency response function matrix, which is measured between the tool tip and the actuation point (see Fig. 1). Then the robust stability boundaries based on the structured singular values are calculated with respect to the uncertainty of the dynamics. The results are presented in a case study with real measured frequency response functions.

2. MODEL OF TURNING OPERATIONS WITH CONTROL

The dynamical model of turning operations including feedback control is presented in Fig. 1. The cutting force $f_1(t)$ acting at the tool tip (associated with coordinate $q_1(t)$) is determined by the formula

$$f_1(t) = K_c w h(t), \tag{1}$$

where K_c is the cutting-force coefficient, w is the depth of cut and $h(t)$ is the instantaneous chip thickness (see Altintas (2012)). Due to the vibrations of the tool, the chip thickness is determined not only by the feed motion, but also by the current and previous positions of the tool one revolution before. For constant spindle speeds, the regenerative time delay can be given explicitly as $\tau_1 = 60/\Omega$, where Ω is the workpiece revolution given in rpm. Then the modified chip thickness is given by the relation

$$f_1(t) = K_c w\big(v_f \tau_1 + q_1(t-\tau_1) - q_1(t)\big), \tag{2}$$

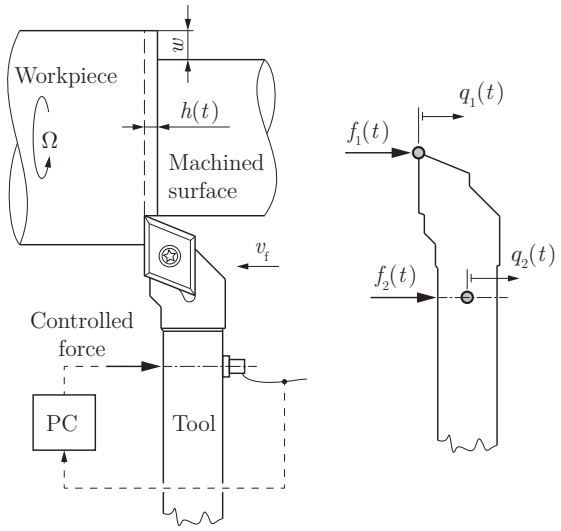

Fig. 1. Dynamical model of turning operations with stabilizing controller.

where v_f is the feed velocity.

When the position and velocity are measured at the actuation point (associated with coordinate $q_2(t)$), the actuator force can be given by the feedback law

$$f_2(t) = -k_p q_2(t-\tau_2) - k_d \dot{q}_2(t-\tau_2), \tag{3}$$

where k_p and k_d are the proportional and the derivative control gains and τ_2 is the inherent feedback delay in the control loop. In order to simplify derivations, the following notation is used

$$\mathbf{f}(t) = \begin{pmatrix} f_1(t) \\ f_2(t) \end{pmatrix} \quad \text{and} \quad \mathbf{q}(t) = \begin{pmatrix} q_1(t) \\ q_2(t) \end{pmatrix}. \tag{4}$$

The transfer function matrix $\mathbf{H}(\omega)$ between the forcing $\mathbf{F}(\omega) = \mathcal{F}(\mathbf{f}(t))$ and displacement $\mathbf{Q}(\omega) = \mathcal{F}(\mathbf{q}(t))$ is defined as

$$\mathbf{H}(\omega)\mathbf{F}(\omega) = \mathbf{Q}(\omega), \tag{5}$$

which in this case can be written as

$$\begin{pmatrix} H_{11}(\omega) & H_{12}(\omega) \\ H_{21}(\omega) & H_{22}(\omega) \end{pmatrix} \begin{pmatrix} F_1(\omega) \\ F_2(\omega) \end{pmatrix} = \begin{pmatrix} Q_1(\omega) \\ Q_2(\omega) \end{pmatrix}. \tag{6}$$

Here, $\mathcal{F}$ denotes the Fourier transformation.

During the stability analysis, the static parts of the forcing can be separated, and only the perturbed motion has to be considered. Assuming that the position vector can be written as $\mathbf{q}(t) = \mathbf{q}_s + \mathbf{x}(t)$, where $\mathbf{q}_s$ is the static deformation and $\mathbf{x}(t)$ is perturbation about the equilibrium, the forcing can be written as

$$\mathbf{f}(t) = \mathbf{f}_s + \mathbf{f}_d(t), \tag{7}$$

where

$$\mathbf{f}_s = \begin{pmatrix} K_c w v_f \tau_1 \\ -k_p q_{s2} \end{pmatrix} \tag{8}$$

and

$$\mathbf{f}_d(t) = \begin{pmatrix} K_c w\big(x_1(t-\tau_1) - x_1(t)\big) \\ -k_p x_2(t-\tau_2) - k_d \dot{x}_2(t-\tau_2) \end{pmatrix}. \tag{9}$$

Taking the Fourier transform of both sides and algebraic manipulations give

$$\mathbf{F}_{\mathrm{d}}(\omega) = \underbrace{\begin{pmatrix} K_{\mathrm{c}} w(\mathrm{e}^{-\mathrm{i}\omega\tau_1} - 1) & 0 \\ 0 & -(k_{\mathrm{p}} + k_{\mathrm{d}}\mathrm{i}\omega)\,\mathrm{e}^{-\mathrm{i}\omega\tau_2} \end{pmatrix}}_{=:\,\mathbf{K}(\omega)} \mathbf{X}(\omega), \tag{10}$$

where $\mathbf{F}_{\mathrm{d}}(\omega) = \mathcal{F}(\mathbf{f}_{\mathrm{d}}(t))$ and $\mathbf{X}(\omega) = \mathcal{F}(\mathbf{x}(t))$.

Substitution of (10) into (5) and simplification with the static terms gives

$$\mathbf{H}(\omega)\mathbf{K}(\omega)\mathbf{X}(\omega) = \mathbf{X}(\omega), \tag{11}$$

$$\big(\mathbf{I} - \mathbf{H}(\omega)\mathbf{K}\,(\omega)\,\big)\mathbf{X}(\omega) = \mathbf{0}. \tag{12}$$

The existence of a periodic solution about the static equilibrium implies that

$$G(\omega; w, \Omega) := \det\big(\mathbf{I} - \mathbf{H}(\omega)\mathbf{K}\,(\omega)\,\big) = 0. \tag{13}$$

In order to construct stability lobe diagram in the plane (Ω, w), (13) can be considered as a co-dimension one problem, where the real and imaginary parts of $G(\omega; w, \Omega)$ give two scalar equations and a one-dimensional curve is sought in the parameter space of Ω, w and ω. The multi-dimensional bisection method developed by Bachrathy and Stepan (2012) is an efficient and fast numerical tool for this task. Note, that the bifurcation curves calculated from the condition (13) separates the space of the machining parameters, where the number of unstable characteristic exponents is constant, but does not identify the stable regions. Identification of stable domains require the application the Nyquist criterion according to Bachrathy and Stepan (2013).

3. ROBUST STABILITY ANALYSIS

3.1 Introduction to μ-analysis

The basic concept of structured singular values was introduced by Doyle (1982) and used to analyze the effect of block-diagonal perturbations of matrices. Since its appearance, it has found many fields of applications, especially in robust control theory with uncertain dynamical properties, see, e.g., Karow et al. (2006).

Let us consider a general matrix $\mathbf{M} \in \mathbb{C}^{m\times n}$, a perturbation set $\mathbf{\Delta}_{\mathrm{s}} \in \mathbb{C}^{n\times m}$ and a given norm $\|\cdot\|$. Then the μ-value of $\mathbf{M}$ is defined as

$$\mu(\mathbf{M}) = \left(\inf\left\{\|\mathbf{\Delta}\|,\ \mathbf{\Delta} \in \mathbf{\Delta}_{\mathrm{s}},\ \det\left(\mathbf{I} - \mathbf{\Delta}\mathbf{M}\right) = 0\right\}\right)^{-1}, \tag{14}$$

for details see the work of Doyle (1982) and Karow et al. (2006). There exist many numerical techniques to obtain μ, however, due to the complexity of the solutions, the calculation time can get significantly high. Formulas for the calculation of μ in case of complex perturbations are presented by Hinrichsen and Pritchard (2005); Packard and Doyle (1993), and for real cases by Hinrichsen and Pritchard (2005) and Qiu et al. (1995), just to mention a few.

In order to provide a simple formula for the characterization of the robustness of turning operations including delayed feedback control, the results of Karow et al. (2006) are applied.

Let us introduce a weight matrix $\mathbf{R} = [R_{jk}]$, $R_{jk} \geq 0$, $\forall\, j, k$ (non-negative matrix) and a weighted maximum norm defined as

$$\|\mathbf{\Delta}\| := \max_{j,k} R_{jk}^{-1} |\Delta_{jk}|. \tag{15}$$

In this case the following equivalence holds for $\mathbf{\Delta}$

$$\|\mathbf{\Delta}\| \leq 1 \quad \Leftrightarrow \quad |\Delta_{jk}| \leq R_{jk},\ \forall\, j, k. \tag{16}$$

Then an upper bound of μ-values can be given by the relations

$$\mu(\mathbf{M}) = \max_{\|\mathbf{\Delta}\|} \rho\left(\mathbf{\Delta}\mathbf{M}\right) \leq \rho\left(\mathbf{R}\tilde{\mathbf{M}}\right) = \rho\left(\tilde{\mathbf{M}}\mathbf{R}\right), \tag{17}$$

where ρ denotes the spectral radius, and $\tilde{\mathbf{M}}$ is a non-negative matrix with $\tilde{M}_{jk} = |M_{jk}|$ (see Karow et al. (2006)).

Detailed derivations, theorems and proofs related to the topic can be found in Karow et al. (2006). An important note is that the inequality in (17) is actually an equality if $\mathbf{M}$ is a diagonal matrix.

A similar application of structured singular values for machining operations was presented by van Dijk et al. (2010), where the spindle speed and depth of cut were assumed to be uncertain and a robust controller was designed. In the current paper the machining parameters are fixed, and only the dynamical behavior is assumed to be uncertain. Moreover, in contrast with van Dijk et al. (2010) the μ-values are approximated by (17) and no D-K iteration is required (see Doyle (1982)).

3.2 Analysis of turning with delayed feedback

Linear dynamical properties of mechanical systems are often determined from impact or shaking tests. In case of machining operations, this requires the accurate excitation of the tool at different points, while the response is measured simultaneously. The measurements are always loaded by noise, which modifies the output, moreover, imperfect excitation can also significantly affect the measured signals. Case studies are presented by Kim and Schmitz (2007), where the uncertainties of the measured frequency response functions are analyzed.

In the uncertain model, it is assumed that the frequency response function matrix is perturbed, where uncertainty of $\mathbf{H}(\omega)$ is modeled by $\mathbf{\Delta}(\omega)$, ie.

$$\mathbf{H}(\omega) \to \mathbf{H}(\omega) + \mathbf{\Delta}(\omega). \tag{18}$$

Modification of the transfer function matrix can be substituted into (12), which directly yields

$$\Big(\mathbf{I} - \big(\mathbf{H}(\omega) + \mathbf{\Delta}(\omega)\big)\mathbf{K}\,(\omega)\,\Big)\mathbf{X}(\omega) = \mathbf{0}. \tag{19}$$

Bringing the uncertain term to the right-hand-side, one obtains

$$\big(\mathbf{I} - \mathbf{H}(\omega)\mathbf{K}\,(\omega)\,\big)\mathbf{X}(\omega) = \mathbf{\Delta}(\omega)\mathbf{K}\,(\omega)\,\mathbf{X}(\omega), \tag{20}$$

where rearrangement gives

$$\mathbf{X}(\omega) = \big(\mathbf{I} - \mathbf{H}(\omega)\mathbf{K}\,(\omega)\,\big)^{-1}\mathbf{\Delta}(\omega)\mathbf{K}(\omega)\mathbf{X}(\omega). \tag{21}$$

If (13) does not hold, then the inverse of $(\mathbf{I} - \mathbf{H}(\omega)\mathbf{K}\,(\omega))$ exists. However, if the determinant is zero, then the parameter point lies on a bifurcation curve, where the system is not robustly stable since an infinitely small perturbation may already destabilize the system.

In order to obtain a standard form, let us introduce the new variable $\mathbf{Z}(\omega)$, such that

$$\mathbf{Z}(\omega) = \mathbf{K}(\omega)\mathbf{X}(\omega). \tag{22}$$

Then some algebraic manipulation, similarly to (13), gives the condition for a bifurcation curve including perturbation

$$\det\left(\mathbf{I} - \underbrace{\mathbf{K}(\omega)\big(\mathbf{I} - \mathbf{H}(\omega)\mathbf{K}(\omega)\big)^{-1}}_{=:\,\mathbf{M}(\omega)}\boldsymbol{\Delta}(\omega)\right) = 0 \tag{23}$$

This is the standard formula for the $\mathbf{M\Delta}$ structure, thus, the method presented in the previous subsection can be applied. Note that the order of the multiplication of matrices $\mathbf{M}(\omega)$ and $\boldsymbol{\Delta}(\omega)$ in (23) can be changed since it does not change the determinant.

According to (17), an upper bound can be given on the structured singular values as a function of the frequency as

$$\mu\big(\mathbf{M}(\omega)\big) < \rho\left(\tilde{\mathbf{M}}(\omega)\mathbf{R}(\omega)\right), \tag{24}$$

where

$$\tilde{M}_{jk}(\omega) = |\mathbf{K}(\omega)\big(\mathbf{I} - \mathbf{H}(\omega)\mathbf{K}(\omega)\big)^{-1}|_{jk}, \tag{25}$$

$$R_{jk}(\omega) = \max\big(|\Delta_{jk}(\omega)|\big). \tag{26}$$

Indeed, $\mathbf{R}(\omega)$ is the matrix of the absolute values of the perturbation bounds.

The so-called stability radius can be introduced as a measure to define the distance from instability (see Karow et al. (2006)) as

$$r^{\mathbb{C}} = \left(\sup_{\omega\geq 0}\mu\big(\mathbf{M}(\omega)\big)\right)^{-1}. \tag{27}$$

Note that, based on the definition of μ, it can be shown that $r^{\mathbb{C}} = 0$ at any bifurcation curve and $r^{\mathbb{C}} = 1$ at the robust stability boundary. Also note, that robustness is defined in the unstable region, too, where the number of unstable characteristic exponents are nonzero, but their number does not change under perturbation. In order to find the robust boundary in the stable domain, first the stable regions must be identified.

Since the structured singular values are approximated, definition (27) can be reformulated as

$$r^{\mathbb{C}} > r := \left(\sup_{\omega\geq 0}\rho\left(\tilde{\mathbf{M}}(\omega)\mathbf{R}(\omega)\right)\right)^{-1}. \tag{28}$$

Here, r refers to lower estimation of the stability radius $r^{\mathbb{C}}$, meaning that the estimation is conservative. By evaluating $r = r(\Omega, w, k_{\mathrm{p}}, k_{\mathrm{d}})$ at some fixed parameter values, it can be determined if the parameter point is robust ($r < 1$) or not ($r > 1$). Similarly, by sweeping a parameter between given bounds, the robust stability boundaries can be found by the level curve $r = 1$.

4. CASE STUDY

In practical applications, the frequency response function measurements are performed multiple times and their average is used during the stability calculations. In this case study, a turning tool was measured 25 times at the tool tip and half way between the tip and the tool holder. The measured frequency response functions and their average is presented in Fig. 2, where the individual

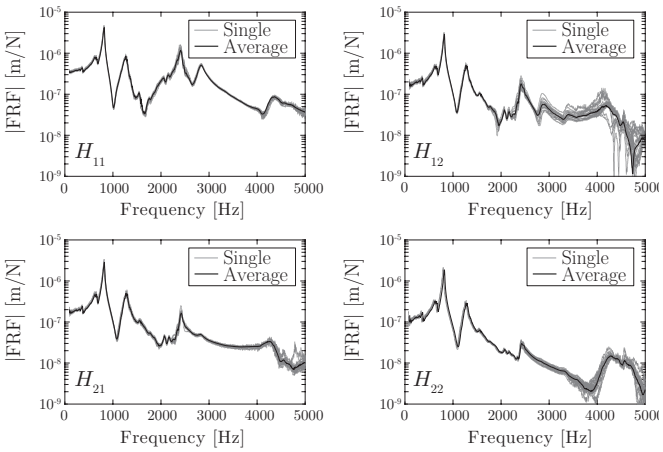

Fig. 2. Measured frequency response functions.

FRFs are plotted by gray solid lines and black solid line indicates their average. The uncertainty is approximated with the standard deviations of the measurements, ie.

$$R_{jk}(\omega) = \sigma\big(H_{jk}(\omega)\big), \tag{29}$$

where $0 \leq R_{jk}(\omega) \in \mathbb{R}$.

Stability lobe diagrams were calculated using the following parameters. The cutting-force coefficient of the workpiece material is $K_{\mathrm{c}} = 363$ MPa and the theoretical chip thickness is $h_0 = v_{\mathrm{f}}\tau_1 = 0.1$ mm. The delay of the controller is assumed to be $\tau_2 = 1$ ms.

The stability diagrams of the coupled system can be plotted in the four-dimensional space of the parameters Ω, w, k_{p} and k_{d}. In order to illustrate the effect of the different parameters, either the machining parameters or the control gains are fixed, while the other two are varied on a fixed interval. These stability diagrams can be considered as two-dimensional projections of the four-dimensional parameter space.

In Fig. 3 (a1-a2), the control gains are set to zero, i.e. the stability lobe diagram of the uncontrolled system is calculated. By evaluating condition (28), the robust stability boundaries can be found. The conventional stability lobe diagram is plotted by solid thin line, while the robust boundary is indicated by solid thick black line. Here, the parameter point P ($\Omega = 3400$ rpm, $w = 1$ mm) results an unstable machining operation. In order to stabilize the machining process at this point, the control gains should be adjusted according to Fig. 3 (a2), where the stability diagram of the controller associated with point P is presented in the plane of the control parameters (in panel (a2) 's' stands for 'stable', 'u' stands for 'unstable' and 'rs' stands for robustly stable). Similarly to the stability lobe diagrams, the robust control parameters can also be found by evaluating condition (28). The conventional (not necessarily robust) stable domain is indicated by light gray shading, while the robust stable region is indicated by dark gray shading and solid thick black line.

The approximation of the μ-values gives an upper estimation of the robust stability boundaries, while the single standard deviation of the measured transfer functions gives a lower estimation of the uncertainties. The interplay of these two counteractive approximations may result either in underestimation or in overestimation of the robust

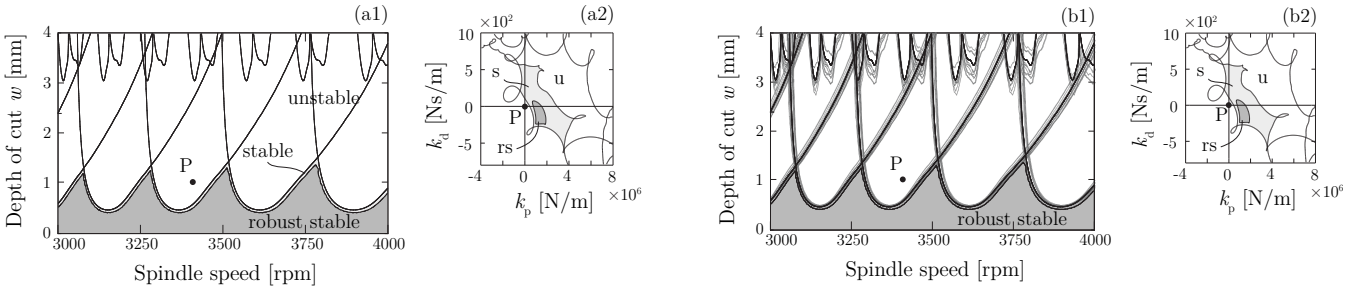

(a) Robust stability boundaries.

(b) Validation by random measured FRFs.

Fig. 3. Robust stability diagram without control ($k_\mathrm{p} = 0$ N/m, $k_\mathrm{d} = 0$ Ns/m).

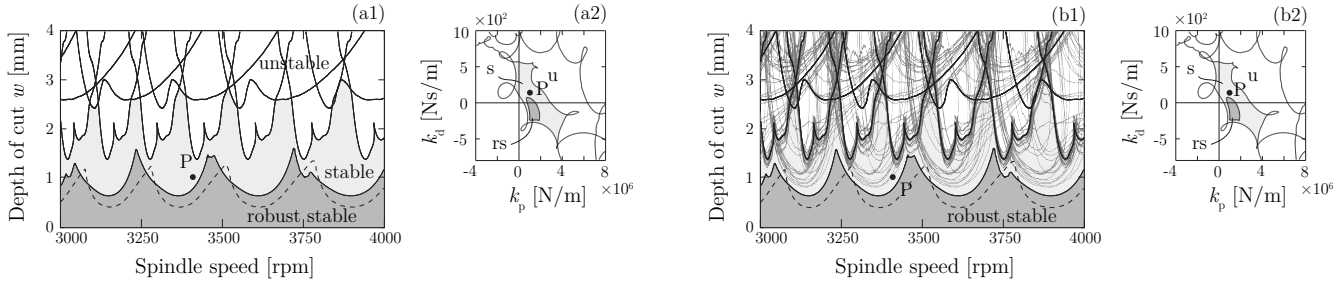

(a) Robust stability boundaries.

(b) Validation by random measured FRFs.

Fig. 4. Robust stability diagram with stable control ($k_\mathrm{p} = 10^6$ N/m, $k_\mathrm{d} = 150$ Ns/m).

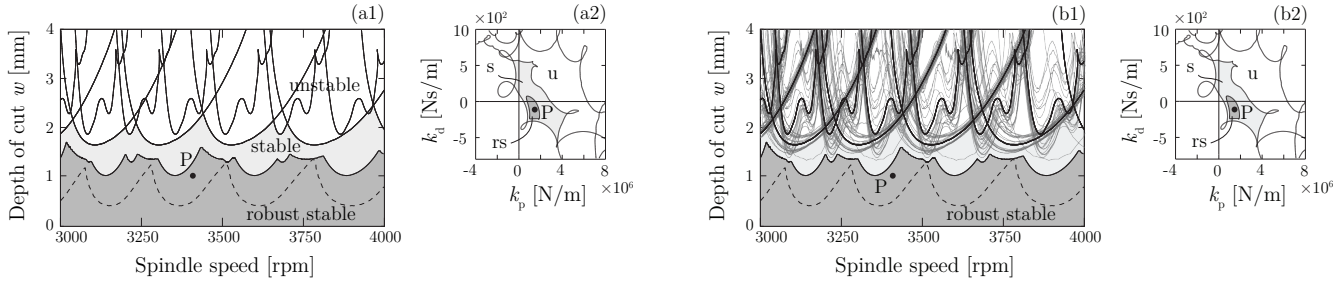

(a) Robust stability boundaries.

(b) Validation by random measured FRFs.

Fig. 5. Robust stability diagram with robust stable control ($k_\mathrm{p} = 1.4 \times 10^6$ N/m, $k_\mathrm{d} = -100$ Ns/m).

stability boundaries. In order to validate the calculations, stability boundaries associated with thirty different random combinations of different measured FRFs are presented in Fig. 3 panel (b1). The boundaries corresponding to the individual FRFs are shown by gray solid lines, while the robust boundary is indicated by solid thick black line. The sensitivity of the stability lobe diagrams is not significant, both the predicted robust boundary and the validated boundary based on random FRF combinations provide a similar solution.

If the designed control parameters give a stable but not robustly stable system, then the machining operation may lose stability under perturbations of the frequency response functions because the uncertainty of the transfer function matrix affects the stability of the closed loop system. In Fig. 4 (a1-a2) the stability lobe diagrams and the control parameters are plotted corresponding to the parameter point P (projections of the four-dimensional parameter space). The designed controller with gains $k_\mathrm{p} = 10^6$ N/m and $k_\mathrm{d} = 150$ Ns/m results in a stable but not robustly stable system. It can be seen in panel (a1) that the uncertain region (light gray shading) significantly increases. Here, dashed line indicates the robust stability boundary of the uncontrolled system, while solid thick black line indicates the robust stability boundary of the closed loop system with the stable controller. It can also be seen that the robust stable domain does not increase significantly.

Similarly to the uncontrolled case, the robust stability lobe diagram can be validated by random FRF combinations, see Fig.4 (b1-b2). As it can be seen, none of the perturbed bifurcation curve crosses the robust boundary, which means that the estimation is still conservative. Also note that the envelopes of the averaged FRFs are calculated from the standard deviations, therefore some of the perturbed stability boundaries may still intersect the predicted robust stability boundary. However, the probability of the worst-case scenarios is significantly smaller,

therefore taking only the single standard deviations was found to be a sufficient approximation in this case study.

The stability lobe diagrams associated with a controller assuring robust stability is shown in Fig. 5 panel (a1-a2). The robust control gains are $k_{\mathrm{p}} = 1.4 \times 10^6$ N/m and $k_{\mathrm{d}} = -100$ Ns/m. Note, that in this case the robust stable region (dark gray shading) gets larger while the uncertain region (light gray shading) slightly shrinks. Parameter point P here lies in the robust stable region. The validation is presented in Fig. 5 (b1).

5. CONCLUSION

Prediction of machine tool chatter involves several uncertain factors, such as the force model or dynamical parameters. Dynamic behavior of the machine tool is characterized by a series of measured frequency response functions, which involves measurement noise, incorrect excitation and variation in the modal parameters. In this paper an active controller-based solution is analyzed, where the control gains are designed in frequency domain based on stability lobe diagrams. Since uncertainty can significantly affect the design of the control parameters, a robust stability analysis method is proposed based on the structured singular values (μ-values). During the calculation, only the measured frequency response functions and their uncertainty are needed. The efficiency and industrial competitiveness of the method are validated in a real case study. It was shown that the standard deviation of the complex frequency response functions can be used as the radius of uncertainty for the robust calculations.

ACKNOWLEDGEMENTS

The research leading to these results has received funding from the European Research Council under the European Unions Seventh Framework Programme (FP/2007-2013) / ERC Advanced Grant Agreement n. 340889, and it was also supported by the ÚNKP-16-3-I. New National Excellence Program of the Ministry of Human Capacities.

REFERENCES

Aguirre, G., Gorostiaga, M., Porchez, T., Munoa, J., 2013. Self-tuning dynamic vibration absorber for machine tool chatter suppression. 28th Annual Meeting of the American Society for Precission Engineering (ASPE).

Altintas, Y., 2012. Manufacturing Automation - Metal Cutting Mechanics, Machine Tool Vibrations and CNC Design, Second Edition. Cambridge University Press, Cambridge.

Bachrathy, D., Stepan, G., 2012. Bisection method in higher dimensions and the efficiency number. Periodica Polytechnica Mechanical Engineering 56 (2), 81–86.

Bachrathy, D., Stepan, G., 2013. Improved prediction of stability lobes with extended multi frequency solution. CIRP Ann - Manuf Techn 62, 411–414.

Doyle, J., 1982. Analysis of feedback systems with structured uncertainties. IEE Proc. 129, Part D., 242–250.

Hajdu, D., Insperger, T., Stepan, G., 2016. Robust stability analysis of machining operations. The International Journal of Advanced Manufacturing Technology.

Hinrichsen, D., Pritchard, A. J., 2005. Mathematical Systems Theory I. Modelling, State Space Analysis, Stability and Robustness. Vol. 48. Springer-Verlag, Berlin.

Huang, X., Hu, M., Zhang, Y., Lv, C., 2016a. Probabilistic analysis of chatter stability in turning. Int J Adv Manuf Technol 87.

Huang, X., Zhang, Y., Lv, C., 2016b. Probabilistic analysis of dynamic stability for milling process. Nonlinear Dynamics 86.

Karow, M., Hinrichsen, D., Pritchard, A. J., 2006. Interconnected systems with uncertain couplings: explicit formulae for μ-values, spectral value sets and stability radii. SIAM Journal on Control and Optimization 45 (3), 856 – 884.

Kim, H. S., Schmitz, T., 2007. Bivariate uncertainty analysis for impact testing. Measurement Science and Technology 18, 3565–3571.

Lehotzky, D., Insperger, T., 2012. Stability of turning processes subjected to digital pd control. Periodica Polytechnica Mechanical Engineering 56 (1), 33–42.

Löser, M., Großmann, K., 2016. Influence of parameter uncertainties on the computation of stability lobe diagrams. In: 7th HPC 2016 CIRP Conference on High Performance Cutting. Vol. 46. Procedia CIRP, pp. 460–463.

Packard, A., Doyle, J. C., 1993. The complex structured singular value. Automatica 29 (1), 71–109.

Park, S., Qin, Y., 2007. Robust regenerative chatter stability in machine tools. Int J Adv Manuf Technol 33, 389–402.

Qiu, L., Bernhardsson, B., Rantzer, A., Davison, E. J., Young, P. M., Doyle, J. C., 1995. A formula for computation of the real stability radius. Automatica 31 (6), 879–890.

Segalman, D., Butcher, E., 2000. Suppression of regenerative chatter via impedance modulation. Journal of Vibration and Control 6 (2), 243–256.

Sims, N. D., 2007. Vibration absorbers for chatter suppression: A new analytical tuning methodology. Journal of Sound and Vibration 301, 592–607.

Tlusty, J., Spacek, L., 1954. Self-excited vibrations on machine tools. Nakl. CSAV, Prague. in Czech.

Tobias, S., 1965. Machine-tool Vibration. Blackie, Glasgow.

Totis, G., 2009. RCPM - a new method for robust chatter prediction in milling. International Journal of Machine Tools and Manufacture 49, 273–284.

van de Wouw, N., van Dijk, N., Nijmeije, H., 2015. Pyragas-type feedback control for chatter mitigation in high-speed milling. pp. 334–339.

van Dijk, N., van de Wouw, N., Doppenberg, E., Oosterling, H., Nijmeijer, H., 2010. Chatter control in the high-speed milling process using μ-synthesis. American Control Conference, 6121–6126.

van Dijk, N., van de Wouw, N., Nijmeijer, H., Faassen, R., Doppenberg, E., Oosterling, J., 2008. Real-time detection and control of machine tool chatter in high speed milling. 2nd International Conference Innovative Cutting Processes and Smart Machining.